

RF AND ACCELERATING STRUCTURE OF 12 MEV UPC RACE-TRACK MICROTRON*

Yu.A. Kubyshev[#], X. Gonzalez, G. Montoro, Technical University of Catalonia, Barcelona, Spain
 D. Carrillo, L. Garcia-Tabares, F. Toral, CIEMAT, Madrid, Spain
 S. Mathot, CERN, Geneva, Switzerland
 V.I. Shvedunov, SINP MSU, Moscow, Russia

Abstract

We describe the design and technical characteristics of a C-band SW accelerating structure of a 12 MeV race-track microtron, which is under construction at the Technical University of Catalonia, and its RF system with a 5712 MHz magnetron as a source. Results of cold tests of the accelerating structure, before and after the brazing, and of high-power tests of the RF system at a special stand are reported. The main features of the magnetron frequency stabilization subsystem are also outlined.

INTRODUCTION

A compact race-track microtron (RTM) with the maximal output energy 12 MeV is under construction at the UPC in collaboration with CIEMAT (Madrid) and the Skobeltsyn Institute of Nuclear Physics (SINP) of the Moscow State University. The design of the accelerator is described in [1] and the course of its development was reported in [2]. The main parameters of the machine are given in Table 1.

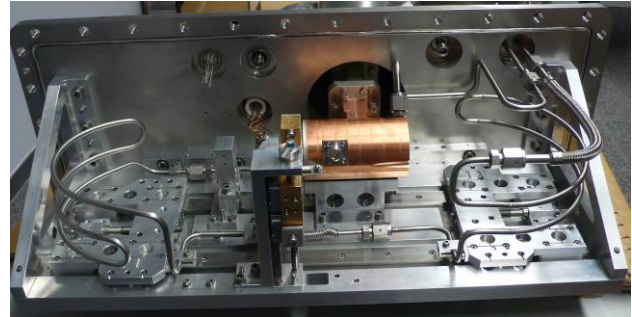
Table 1: RTM parameters

Parameter	Value
Beam energies	6, 8, 10, 12 MeV
Operating frequency	5712 MHz
Synchronous energy gain	2 MeV
Pulsed beam current at RTM exit	5 mA
End magnets field	0.8 T
Injection kinetic energy	25 keV
Pulsed RF power	<750 kW
RTM head external dimensions	670×250×210mm
RTM head weight (including platform and vacuum chamber)	< 100 kg

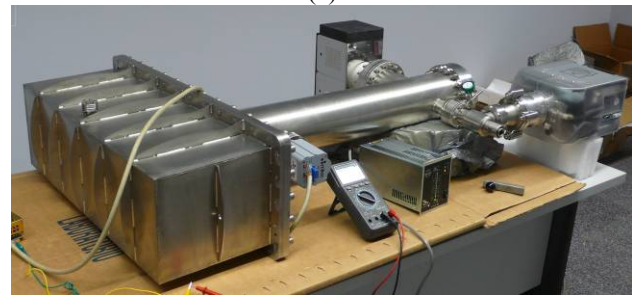
Recently the accelerating structure of the RTM has been brazed and installed, together with other components of the accelerator head, at the common supporting platform (see Fig. 1a). The platform has been placed inside the vacuum chamber and its vacuum tests have been carried out (see Fig. 1b). In parallel first high power tests of the modulator and the magnetron have been performed. In the present article we report on the status and measurements of characteristics of the accelerating structure and tests of the RF system.

*Work supported by the grants VALTEC09-2-0035 of CIDEM and 2009 SGR 1516 of AGAUR (both of the Generalitat of Catalonia) and FPA2010-11911-E of MICINN.

[#]iouri.koubychine@upc.edu



(a)



(b)

Figure 1: (a) Accelerating structure fixed on the supporting platform; (b) Vacuum chamber and pumping tube assembly with the vacuum pumps and vacuum window already connected to it.

ACCELERATING STRUCTURE

The linac of the compact 12 MeV RTM is an on-axis coupled standing wave bi-periodic C-band structure. In [1] the main arguments for the choice of the operating frequency are explained and its main features are described. The linac is composed of one short ($\beta = 0.5$) accelerating cell, optimized for an efficient capture of 25 keV beam from the electron gun, three $\beta = 1$ accelerating cells and three intermediate coupling cells. Its 3D model is shown in Fig. 2. Results of its 2D and 3D design optimization with the HFSS code [3] are reported in [4]. The external front wall of the linac from the side of the short cell plays the role of the anode of the electron gun which was successfully designed and tested [5, 6]. The RF power is provided to the linac via an iris in a WR187 waveguide attached to the $\beta = 1$ cell. The length of the iris was optimized for the coupling factor $\beta_c = 2$ to provide stable linac operation under beam loading. A coupling loop installed in the adjacent $\beta = 1$ cell (see Fig. 2) is used for the control of the accelerating field level, as well for magnetron frequency stabilization as described below.

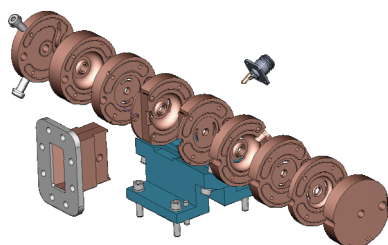


Figure 2: 3D linac model.

Before the machining and brazing of the cells of the accelerating structure two sets of test cells have been machined and tested. The first set is described in [2].

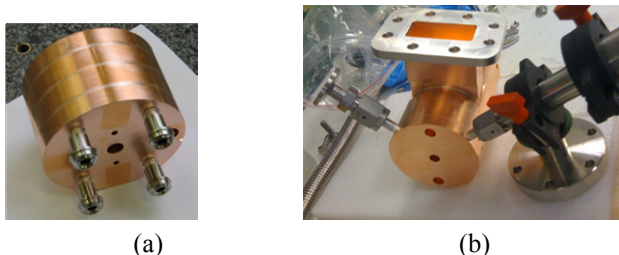


Figure 3: (a) Second test cavity after brazing; (b) Leakage test of the linac cooling system after linac brazing.

The second set of test cavities has been designed and machined with the aim to study the RF properties change after the brazing of the cells. This was a structure consisting of four OFE copper segments which include two half accelerating cells with $\beta = 1$ and one coupling cell with coupling slots. The parts (Fig. 3(a)) have been brazed at CERN with the eutectic alloy Cu28%Ag72%. In the applied brazing procedure the melting point was exceeded for less than two minutes with the maximum temperature being 786°C. Measurements performed before and after the brazing have shown that the change of the resonant frequency was only 0.03%. The value of the unloaded Q_0 factor was higher than 90% of the value obtained in the design simulations.

In the view of the quite satisfactory results in case of the second test structure it has been decided to follow the same machining and brazing procedures in the case of the final version of the linac. As a first step, a rough machining has been done. Afterwards the parts were subjected to an internal stresses release procedure followed by the fine machining to obtain the final geometry. Measurements performed before the brazing at a pressure test stand have shown that there is a good agreement with the simulations. In particular, the theoretical and experimental dispersion characteristics practically coincide and the resonant frequency of the acceleration mode is 0.04% below the theoretical one. In order not to cause plastic deformations of the copper segments pressure applied at the hydraulic press was rather low, as a result the measured quality factor Q_0 was 78% of the theoretical value.

The brazing of the linac has been carried out also at CERN. A leakage test of its cooling system performed after the brazing (see Fig. 3 (b)) has shown that no leakage at level 10^{-12} mbar.l.s⁻¹ has been detected.

Measurements of RF characteristics have shown that the quality factor of the brazed structure is higher than 95% of the design value (see Table 2). The resonant frequency of the accelerating mode increased only by 0.01%, however the adjacent modes have shifted more, likely because of some internal stress release due to the thermal heating at high temperature (Fig. 4(a)).

The electric field profile on the axis has been measured by means of a bead-pull test with a 0.6 mm thick metallic disc. As one can see in Fig 4(b) the theoretical E-field and the field profiles measured before and after the brazing all are quite close to each other and no field in the coupling cells has been detected. The measured waveguide-linac coupling factor is about 25% less than the calculated one. This is partially explained by the value of the quality factor lower than the theoretical one, this is due to the cells surface roughness and can be adjusted by increasing the iris length.

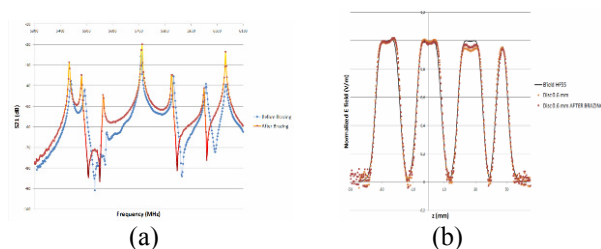


Figure 4: (a) Linac resonant frequencies and (b) E-field before (blue line) and after (red line) the brazing

Table 2: Experimental and theoretical values of the accelerating structure electromagnetic characteristics

	Q_0	β_c	f (MHz)
Experimental value	9075	1.50	5713.5
Theoretical value	9493	2.0	5714.1

RF SYSTEM

The RF source of the RTM is a C-band (5.45-5.85GHz) CPI 1 MW coaxial air cooled magnetron SFD-313V. It is powered by a ScandiNova M1 2MW solid state switched magnetron modulator. The modulator-magnetron assembly provides about 1MW/1kW pulsed/average RF power at 5712 MHz in 3 μ s length pulses following with the repetition rate up to 250 Hz.

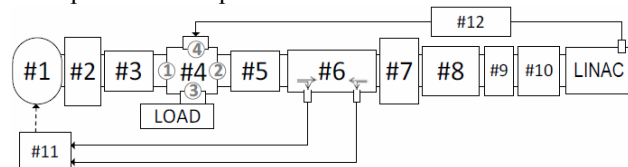


Figure 5: RTM RF system elements.

The RTM RF system architecture is shown in Fig. 5. The RF power is transmitted from the magnetron (1) to the linac via the following series of WR187 elements: flexible waveguide (2), pressure unit (3), four-port circulator with terminations (4), H-bend with arc detector (5), dual loop coupler (6), rotary joint (7), vacuum window (8), and rigid (9) and flexible (10) waveguides.

The matching of the magnetron frequency to the linac one is achieved by means of an Automatic Frequency Control (AFC) system (11) and a Low Power RF (LPRF) control (12). The function of the circulator is to protect the magnetron from the reflected RF power and also to forward the signal from the linac coupling loop to the magnetron entrance. The arc detector stops the modulator trigger signal when discharges inside the waveguide are produced. The non-vacuum part of the waveguide tract is filled with SF₆ gas at 2 bar pressure to prevent arcing. Main parameters of the RF system are summarized in Table 3.

There are several phenomena which lead to a mismatch between the frequency of the RF power generated by the magnetron and the accelerating structure resonance frequency. These are: slow drift of the magnetron body temperature, slow and fast magnetron current instabilities, a drift of the accelerating structure resonance frequency during the start-up due to the structure heating and deformations and also during the following operation due to the variation of the cooling water temperature. This mismatch between the frequencies produces a reflected RF wave and causes instability of the accelerating field level. The slow drift is compensated by the AFC system which compares the direct and reflected RF signals extracted from the dual loop coupler by means of a phase detector and generates an error signal activating a stepper motor for mechanical adjustment of the magnetron frequency. For the fast but short-term frequency variation (less than 2 MHz) another adjusting mechanism is used, namely the RF signal extracted from the linac via the control loop passes through the LPRF system, is injected into port 4 of the four-ports circulator and pulls the magnetron frequency to the linac resonant value.

Table 3. The RF system operation parameters

Parameter	Value
Operating frequency	5712 MHz
RF and E-gun pulse length	3 μ s
Pulse repetition rate	1-250 Hz
Magnetron anode voltage	36 kV
Magnetron anode current	60 A
Modulator output pulse power	2.2 MW
Magnetron output pulse power	\leq 1 MW
Waveguides insulation	SF ₆ (2 bar)

RF TESTS

The RF power generation has been tested at an RF test stand (Fig. 6a). In this case the magnetron fed by the modulator transmits the wave through a line consisting of the flexible waveguide, pressure unit and dual loop coupler, to a water cooled load. The direct signal from the dual loop coupler can be sent to a powermeter or through a diode to an oscilloscope. Generated pulses are shown in

Fig. 6 (b). The RF average power can be estimated from the power measured by a powermeter using known directional coupler parameters or by the difference between the temperatures of cooling water at the entrance and exit of the load. The pulsed power is calculated using the measured duty factor. Preliminary measurements by these two methods give the value of the pulse power 700-800 kW.

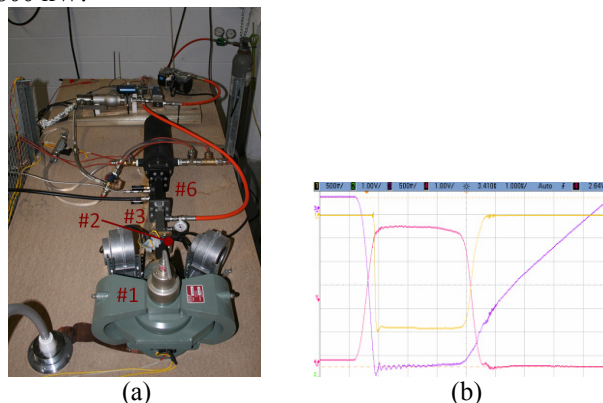


Figure 6: (a) Microtron RF stand, the elements numbering corresponds to the one in Fig. 5a. (b) Pulses generated in the RF tests: voltage supplied to Magnetron (violet, 1V:10kV), current (pink, 0.1V:1A), RF signal obtained from RF diode (yellow).

CONCLUSIONS

Two important steps have been done on the way to high power tests of UPC RTM linac: (1) it had been brazed and cold RF measurements have been done demonstrating satisfactory results; and (2) magnetron and modulator operation has been tested and RF power close to project value measured.

REFERENCES

- [1] A.P. Poseryaev, V.I. Shvedunov, M. Ferrer Ballester and Yu.A. Kubyshev, "Design of 12 MeV RTM for multiple applications", EPAC'06, Edinburgh, June 2006, WEPCH175, p. 2340 (2006).
- [2] Yu.A. Kubyshev et al. "Current Status of the 12 MeV UPC Race-Track Microtron", PAC'09, Vancouver, May 2009, WE6PFP112, p. 2775 (2009).
- [3] <http://www.ansoft.com>
- [4] Yu. Kubyshev, D. Carrillo, L. García-Tabarés, F. Toral, A. Poseryaev, V. Shvedunov, "C-band Linac Optimization for a Race-Track Microtron", EPAC'08, Genoa, June 2008, MOPP096, pp. 778 (2008).
- [5] A.V. Alov, D. Carrillo, Yu.A. Kubyshev, N.I. Pakhomov, and V.I. Shvedunov, NIM A 624 (2010) p. 39.
- [6] Yu. Kubyshev, A.V. Alov, V.I. Shvedunov, N.I. Pakhomov, "A novel electron gun for off-axis beam injection". To appear in the Proceedings of PAC'11, New York, March-April, 2011, WEP290.